

# Emergent $O(4)$ symmetry at an one-dimensional deconfined quantum tricritical point

**Ning Xi**

Department of Physics and Beijing Key Laboratory of Opto-electronic Functional Materials and Micro-nano Devices, Renmin University of China, Beijing 100872, China

**Rong Yu**

Department of Physics and Beijing Key Laboratory of Opto-electronic Functional Materials and Micro-nano Devices, Renmin University of China, Beijing 100872, China

E-mail: [rong.yu@ruc.edu.cn](mailto:rong.yu@ruc.edu.cn)

**Abstract.** We show an  $O(4)$  symmetry emerges at a deconfined quantum tricritical point of a valence bond solid and two ferromagnetic phases in an  $S = 1/2$  frustrated spin chain by combining analytical analysis and numerical calculations with the time evolution of infinite matrix product states. With this symmetry the valence-bond solid and the three magnetic order parameters form an  $O(4)$  pseudovector in the infrared limit, and can continuously rotate into each other. We numerically determine the location of the quantum tricritical point and study the scaling of the correlation functions of the  $O(4)$  vector components and associated conserved currents. The critical behaviors of these correlation functions are all in accord with field theoretical results. The emergent  $O(4)$  symmetry at the tricritical point is justified by the integer value of the scaling dimension of the emergent Noether conserved currents. Our findings not only give direct evidence of such a high emergent symmetry at an one-dimensional valence bond solid to magnetic transition but also shed light on exploring emergent symmetries in higher dimensions.

*Keywords:* One-dimensional antiferromagnetism, spin frustration, deconfined quantum critical point, emergent symmetry, infinite time-evolving block decimation

## 1. Introduction

Quantum phase transitions (QPTs) in spin systems are usually accompanied by abundant emergent phenomena, including unconventional spin dynamics, fractionalized excitations, topological excitations, and enhanced symmetry [1–14]. Among these, the origin of emergent enhanced continuous symmetry at the transition point is one intriguing theme that has been extensively investigated [11–21].

As one promising theory, the theory of deconfined quantum critical point (DQCP) successfully predicts the existence of emergent continuous symmetry at the continuous transition between two spontaneous symmetry breaking (SSB) phases in two-dimensional (2D) systems [13, 22–24]. At the DQCP, besides the emergent deconfined fractionalized spin excitations, the enhanced symmetry allows continuous rotation between the order parameters of the two ordered phases [25–28]. For example, an emergent  $SO(5)$  symmetry has been observed numerically at the DQCP between the antiferromagnetic (AFM) and valence bond solid (VBS) states on the 2D square lattice [14, 15, 29].

The development of the DQCP theory sheds light on understanding the emergent symmetry at the VBS to magnetic transition. However, it is sufficient but not necessary for the emergent symmetry at a phase transition. For instance, evidences of enhanced continuous symmetry at first-order transitions between AFM and VBS phases are recently reported [16, 20]. In these systems the origin of the emergent symmetry remain elusive.

Despite the complex situation in high dimensional systems, the emergent continuous symmetry in 1D systems is more accessible. This is not only because more controllable analytical and numerical tools are available, but also because the significant quantum fluctuations in 1D systems constrains the type of transition. This is especially true for the systems where the Lieb-Schultz-Mattis (LSM) theorem holds. For example, in an  $S = 1/2$  chain with spin rotational and lattice translational symmetries, the ground state either breaks the translational symmetry to form a VBS state or keeps plainly gapless with the symmetries preserved [30]. Therefore, for a LSM system with spin rotational and lattice translational symmetries, a first-order transition with an enhanced continuous symmetry can not take place, and the ground state at the transition point, being gapless, least preserves the symmetries of the underlying Hamiltonian, and may even extend to an enhanced symmetry [30–32]. In other words, the DQCP theory applies to these systems in a more universal way. Recently, some works studied possible DQCP in 1D spin systems and obtained some interesting results. [33–41].

To clarify the nature of the emergent continuous symmetry accompanied by the magnetic-VBS transition in 1D systems, we investigate the QPT of a frustrated spin-1/2 chain. Inspired by the results of an spin-1/2 AFM Heisenberg chain, where the microscopic  $SU(2)$  symmetry extends to an  $SO(4)$  symmetry in the continuous limit [5, 41–44], we show that an  $O(4)$  symmetry emerges at the quantum tricritical point of the VBS and two ferromagnetic (FM) phases in our model. To be specific, the

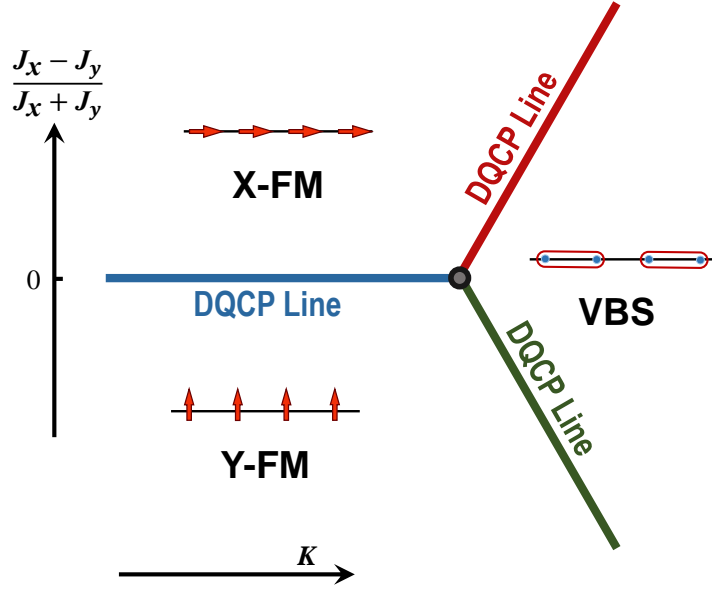


**Figure 1.** A schematic phase diagram for the spin model defined in Eq. 1. The isotropic DQCP line with microscopic U(1) symmetry (blue line) separates the  $X$ -direction and  $Y$ -direction FM phases. The DQCP lines between the FM and VBS phases (red and green line) with emergent  $O(2) \times O(2)$  symmetry have been studied in Ref. [34]. As shown later in this paper, an enhanced  $O(4)$  symmetry emerges at the intersection point of these three quantum critical lines, which is a quantum tricritical point (black point). A more completed phase diagram is described in Ref. [36].

Hamiltonian of our model reads

$$H = \sum_i (-J_x S_i^x S_{i+1}^x - J_y S_i^y S_{i+1}^y) + K (S_i^x S_{i+2}^x + S_i^y S_{i+2}^y). \quad (1)$$

Here  $J_x$  and  $J_y$  refer to nearest-neighbor (n.n.) FM exchange interactions and  $K$  is the next n.n. AFM exchange coupling. The model supports an  $X$ -direction FM, a  $Y$ -direction FM, and a VBS in the ground-state phase diagram, as depicted in Fig. 1.

For  $J_x > J_y$  and small  $K$ , the ground state is a FM with spins ordered along the  $X$ -direction ( $X$ -FM). Likewise, the ground state is a  $Y$ -FM for  $J_x < J_y$  and small  $K$ . The  $X$ -FM and  $Y$ -FM states meet at the isotropic line  $J_x = J_y$  (blue line in Fig. 1) where the spin rotational symmetry of the Hamiltonian is enhanced from  $Z_2^x \times Z_2^y$  to U(1). Across this isotropic line by tuning the parameter  $J_x - J_y$  in the model, the system undergoes a continuous transition, i.e. a line of DQCPs [45]. For sufficiently large  $K$ , the ground state is a VBS that breaks the translational symmetry. It has been proposed that DQCPs with emergent  $O(2) \times O(2)$  symmetry [34] exist along the FM and VBS phase boundary (red and green lines in Fig. 1).

The two  $O(2)$  symmetries between  $X$ -FM ( $Y$ -FM) and VBS respectively correspond to the rotation between the order parameters of VBS and  $X$ -FM ( $Y$ -FM) and the rotation between the order parameters of  $Y$ -FM ( $X$ -FM) and  $Z$ -AFM. Meanwhile, the U(1) symmetry between  $X$ -FM and  $Y$ -FM guarantees the continuous rotation between

these two order parameters. As a consequence, at the tricritical point (black point in Fig. 1), the four order parameters of  $X$ -FM,  $Y$ -FM,  $Z$ -AFM, and VBS are expected to be rotated into each other by an enhanced  $O(4)$  symmetry.

In this work, we present results of analytical analysis and numerical calculations to show an  $O(4)$  symmetry indeed emerges in the infrared limit at the tricritical point of the  $X$ -FM,  $Y$ -FM, and VBS phases. The rest of this paper is organized as follows. In Sec. 2, we review the field theoretical description of this 1D model, from which the emergent  $O(4)$  symmetry is expected. In Sec. 3, we introduce our numerical technique based on the time evolution of infinite matrix product states (MPS) for calculating the correlation functions of  $O(4)$  vector components and associated conserved currents from which the critical exponent  $\eta$  (related to scaling dimensions  $\Delta$ ) for each component is extracted. Then in Sec. 4, we numerically study the transition along the isotropic line and determine the exact location of the tricritical point. In Sec. 5, the emergent  $O(4)$  symmetry and the associated conserved currents correlation at the tricritical point are investigated in detail. We show that the scaling dimensions of all the emergent Noether conserved currents associated with the  $O(4)$  vector are pinned to an integer of  $\Delta = 1$ , which justifies the existence of the emergent  $O(4)$  symmetry.

## 2. Low-energy effective model description

The model of Eq. (1) has been analyzed by using several different approaches [34–37]. Here we adopt a direct bosonization approach which can give a clear understanding of the QPT and emergent symmetries. Following the standard procedure of bosonization [5,37], the low-energy symmetry-preserving bosonized hamiltonian reads as

$$H_b = H_0 + H_{\text{int}}, \quad (2)$$

where

$$H_0 = \frac{v}{2} \int dr \left[ \frac{1}{g} (\partial_r \Theta)^2 + g (\partial_r \Phi)^2 \right], \quad (3)$$

and

$$H_{\text{int}} = \int d\tau dr [\lambda_\Theta \cos(4\Theta) + \lambda_\Phi \cos(2\Phi)]. \quad (4)$$

Here  $v$  is the Fermi velocity, and  $g$  is the Luttinger parameter.  $\lambda_\Theta$  and  $\lambda_\Phi$  are two interaction couplings that can drive the ground state to different orders.  $\Theta$  and  $\Phi$  are two dual bosonic fields whose commutation relation reads as

$$\left[ \frac{\partial_r \Theta(r_1)}{\pi}, \Phi(r_2) \right] = i\delta(r_1 - r_2). \quad (5)$$

The mapping between the spin operators of the microscopic model and the bosonic fields are as follows:

$$\begin{aligned}
S^x(r) &\sim \cos[\Phi(r)], \\
S^y(r) &\sim -\sin[\Phi(r)], \\
S^z(r) &\sim \partial_r \Theta(r) - C_z (-1)^r \sin[2\Theta(r)], \\
\vec{S}(r)\vec{S}(r+1) &\sim (-1)^r \cos[2\Theta(r)].
\end{aligned} \tag{6}$$

Then for small  $H_{\text{int}}$ , one can calculate the scaling dimension  $\Delta$  of the two interaction terms [37]:

$$\begin{aligned}
\Delta[\cos(4\Theta)] &= 4g, \\
\Delta[\cos(2\Phi)] &= 1/g.
\end{aligned} \tag{7}$$

For  $g > 1/2$ , the  $\cos(4\Theta)$  term is relevant and  $\cos(2\Phi)$  term is irrelevant. The ground state will be either a VBS (where  $\Theta = 0$  or  $\pi/2$ ) for  $\lambda_\Theta < 0$  or a Z-AFM (where  $\Theta = \pi/4$  or  $3\pi/4$ ) for  $\lambda_\Theta > 0$ . Likewise, for  $g < 1/2$ , the ground state will be either an X-FM for  $\lambda_\Phi < 0$  or a Y-FM for  $\lambda_\Phi > 0$ . Interestingly, at  $g = 1/2$ , these two interaction terms are both marginally irrelevant and the hamiltonian is symmetric under the  $2\Theta \leftrightarrow \Phi$  interchange for  $\lambda_\Theta = \lambda_\Phi < 0$ . Note that one may rewrite  $\cos(4\Theta)$  to  $\cos^2(2\Theta) - \sin^2(2\Theta)$ , and  $\cos(2\Phi)$  to  $\cos^2(\Phi) - \sin^2(\Phi)$ . This means, at the X-FM to VBS transition point (red line in Fig. 1), there exists a continuously rotation between the order parameters of the X-FM state,  $\cos(\Phi)$ , and the VBS state,  $\cos(2\Theta)$ . Actually, there is an additional rotation between the order parameters of the Y-FM state ( $\sin(\Phi)$ ) and the Z-AFM state ( $\sin(2\Theta)$ ). But a transition between the Z-AFM and VBS states would require  $\lambda_\Theta = 0$  and  $g > 1/2$ , which cannot be satisfied in the original microscopic model of Eq. (1). Similar analysis can be applied to the DQCP between the Y-FM and VBS (green line in Fig. 1) for  $\lambda_\Theta = -\lambda_\Phi < 0$ . Another transition takes place at  $\lambda_\Phi = 0$  and  $g < 1/2$ , corresponding to the DQCP between the X-FM and Y-FM (blue line in Fig. 1).

We investigate the enhanced symmetry at the tricritical point by approaching it along the isotropic line (fixing  $J_x = J_y$  and increasing  $K$  in Eq. (1), or equivalently, fixing  $\lambda_\Phi = 0$  and increasing  $g$  in Eq. (2)). Along this line, the low-energy effective Hamiltonian is simplified to the standard sine-Gordon model. The scaling dimensions and critical behaviors of these bosonic fields and corresponding spin operators can be calculated analytically. It is well known that across the tricritical point from the Luttinger liquid phase (critical line of the X-FM and Y-FM phases) to the VBS phase, the system will undergo a Kosterlitz-Thouless (KT) transition [3, 5, 37, 38, 46, 47].

In light of the scaling dimension analysis aforementioned, all the interaction terms are irrelevant along the isotropic critical line. Therefore, the Hamiltonian  $H_b$  flows to  $H_0$  under renormalization group transformations. It is noteworthy that the  $\cos(4\Theta)$  term at the tricritical point is marginally irrelevant, which will cause a correction to scaling.

At the tricritical point, the effective sine-Gordon model can be rewritten in a fermionic representation defined on bond. The  $\cos(4\Theta)$  term provides an irrelevant

backscattering process corresponding to spin flip on bond [3, 5, 37, 46, 47]. If we ignore the marginally irrelevant interaction, the model is mapped to the  $k = 1$   $SU(2)_1$  Wess–Zumino–Novikov–Witten (WZNW) model [3, 5, 41, 46]:

$$H_{\text{WZNW}} = \int dx \left[ \vec{J}_L \cdot \vec{J}_L + \vec{J}_R \cdot \vec{J}_R \right], \quad (8)$$

where  $\vec{J}_L$  and  $\vec{J}_R$  are the left-move and right-move current operators, respectively. They both satisfy the  $SU(2)_1$  Kac–Moody algebra. Consequently, this WZNW model possessed two independent  $SU(2)$  symmetries. However, the real situation is more complicated because the interaction term will mix the left-move and right-move current. Note that in the infrared limit, the interaction term is irrelevant. This means we should still obtain the WZNW model with two independent  $SU(2)$  symmetries after a proper redefinition of the left- and right-moving modes. Therefore, we expect the symmetry at the tricritical point extends to  $SU(2) \times SU(2) \sim O(4)$ , just like the case in the Heisenberg model [5, 41, 43]. Instead of presenting an analytical proof, in the following, we justify this emergent  $O(4)$  symmetry by numerical calculations on the original microscopic model.

To examine the critical properties of the system, we calculate the correlation functions of the order parameters and the corresponding conserved currents. With the emergent symmetry, the order parameters of X-FM, Y-FM, Z-AFM, and VBS form an  $O(4)$  pseudovector. In terms of microscopic spin operators, the components of the  $O(4)$  pseudovector read

$$\begin{aligned} \text{X-FM} : n_1(r_i) &\sim S_j^x + S_{j+1}^x \\ \text{Y-FM} : n_2(r_i) &\sim S_j^y + S_{j+1}^y \\ \text{Z-AFM} : n_3(r_i) &\sim (-1)^j (S_j^z - S_{j+1}^z) \\ \text{VBS} : n_4(r_i) &\sim (-1)^j \vec{S}_j \cdot \vec{S}_{j+1}. \end{aligned} \quad (9)$$

Moreover, the  $O(4)$  group has six Lie group generators which generates the rotation between any two components of the  $O(4)$  pseudovector. As a consequence, there must be 12 emergent conserved currents labeled as  $\mathcal{J}_{ab}^\mu$ , corresponding to the continuous rotational symmetry of  $n_a$  and  $n_b$  ( $a, b = 1, 2, 3, 4$  and  $a < b$ ) with space-time components labeled by  $\mu = \tau, r$ . In terms of microscopic spin operators, they can be written as

$$\begin{aligned} \mathcal{J}_{12}^r &\sim \mathcal{J}_{34}^r \sim S_j^z + S_{j+1}^z \\ \mathcal{J}_{13}^r &\sim \mathcal{J}_{24}^r \sim (-1)^j (S_j^y - S_{j+1}^y) \\ \mathcal{J}_{23}^r &\sim \mathcal{J}_{14}^r \sim (-1)^j (S_j^x - S_{j+1}^x) \\ \mathcal{J}_{14}^r &\sim \mathcal{J}_{23}^r \sim (-1)^j (S_j^y S_{j+1}^z + S_j^z S_{j+1}^y) \\ \mathcal{J}_{24}^r &\sim \mathcal{J}_{13}^r \sim (-1)^j (S_j^x S_{j+1}^z + S_j^z S_{j+1}^x) \\ \mathcal{J}_{34}^r &\sim \mathcal{J}_{12}^r \sim (S_j^x S_{j+1}^y - S_j^y S_{j+1}^x). \end{aligned} \quad (10)$$

The WZNW model predicts that the scaling dimensions of the conserved currents and the vector components are 1 and 1/2, respectively. The critical exponent  $\eta$  and

the scaling dimension  $\Delta$  are related by  $\eta = 2\Delta$ . However, due to the existence of marginally irrelevant operators, the correlation functions of vector components acquire a multiplicative logarithmic correction and behave as [3, 5, 46, 48]

$$\begin{aligned}\langle n_a(0)n_a(r) \rangle &\sim \frac{\ln^{\frac{1}{2}}(r)}{r}, a = 1, 2, 4 \\ \langle n_3(0)n_3(r) \rangle &\sim \frac{f(r)}{r}.\end{aligned}\tag{11}$$

Here,  $f(r)$  is a weak correction term and would be unimportant for  $r \gg 1$  [48]. Note that the critical behaviour of the correlation functions of the vector components should be in accord with the prediction of the WZNW model only in the infrared limit. For the conserved currents, they should not acquire such corrections to scaling. If the  $O(4)$  symmetry indeed emerges at this point, the conservation law guarantees the scaling dimension of the conserved currents to  $\Delta = 1$ , *i.e.*  $\eta = 2$  and the correlation functions of conserved currents should behave as

$$\langle \mathcal{J}_{ab}^\mu(0)\mathcal{J}_{ab}^\mu(r) \rangle \sim \frac{1}{r^2}.\tag{12}$$

There are only 6 independent microscopic operators in Eq. 10 for the 12 conserved currents with  $\mu = \tau, r$  and  $a, b = 1, 2, 3, 4$ . For simplicity, we denote  $\mathcal{J}_{ab} = \mathcal{J}_{ab}^r$  in the following discussion. The corresponding components  $\mathcal{J}_{ab}^\tau$  can be easily obtained from Eq. (10).

### 3. Numerical Methods

In this work, we adopt a MPS based infinite time-evolving block decimation (iTEBD) [49, 50] method to study the ground-state properties of the spin model defined in Eq. (1). Generally, with sufficiently large Schmidt rank  $D$ , MPS can ensure accuracy only for gapped systems. In the situation where the system is gapless, with various well developed finite- $D$  or finite-entanglement scaling techniques, MPS is capable of exploring the ground-state properties trustingly [51–53]. A finite- $D$  scaling technique will be detailed and applied in the analysis of the KT transition.

A two-point correlator of operators  $u$  and  $v$  in the matrix product representation take the generic form as [50]

$$\langle u(0)v(r) \rangle = \sum_{k=1}^{\text{rank}(D \times D)} c_k (\Lambda_k)^{r-1}.\tag{13}$$

Here,  $\Lambda_k$ s are the eigenvalues of the transfer operator and  $\Lambda_1$  is the largest eigenvalue. If we transform the transfer operator into a normalized form with  $\Lambda_1 = 1$ , there remains a constant term  $c_1$  and an exponential decay term  $\sum c_k \Lambda_k^{r-1}$  in Eq. (13). The constant term guarantees the long range order. The leading decay factor  $\gamma = \Lambda_2$  (the second largest eigenvalue) contributes an effective correlation length as

$$\xi = -1/\ln(|\gamma|).\tag{14}$$

There are two parts in Eq. (13).  $(\Lambda_k)^{r-1}$  terms reflect the intrinsic characteristic of the ground state, while the  $c_k$  terms dictate the specific correlation behaviors for given operators of  $u$  and  $v$  in Eq. (13). Also note that the effective correlation length  $\xi$  is obtained from the second largest eigenvalue, and hence is independent of the correlation function. Furthermore in the situation where the system is gapless (actual correlation length  $\tilde{\xi} \rightarrow \infty$ ), the effective correlation length  $\xi$  would conform to a power law behavior as [52]

$$\xi \sim D^\kappa. \quad (15)$$

Here,  $\kappa$  is the finite-entanglement scaling exponent related to central charge  $c$  as

$$\kappa = \frac{6}{c \left( \sqrt{\frac{12}{c}} + 1 \right)}. \quad (16)$$

Instead, for the gapped system, correlation length is always a finite value, even in the infinite- $D$  limit. Thus, the extrapolations of  $\xi$  in the infinite- $D$  limit can make a distinction between gapped and gapless systems.

To determine a ground state in matrix product representation, one usually starts from a random initialization. Deep inside an ordered phase, the ground state is not sensitive to the way of initialization. The local order parameters and ground-state energy are sufficiently accurate with a finite  $D$ . However, when the system is in a quasi-long-range (QLR) ordered phase, finite- $D$  effects may appear. The gap obtained in a finite- $D$  MPS is always finite which leads to a finite value of order parameters. This long range order is an artifact and will disappear in the infinite- $D$  limit. For example of the ground-state calculation on the isotropic line (blue line in Fig. 1) in this work, the magnetic order parameters  $\langle S^x \rangle$  and  $\langle S^y \rangle$  are always finite values. Moreover, the  $U(1)$  symmetry of Hamiltonian results in infinite degenerate local minima of rotating between  $\langle S^x \rangle$  and  $\langle S^y \rangle$  with finite  $D$ . To eliminate the effects of the finite values of order parameters as much as possible, we fix the obtained magnetic order along one direction and calculate the correlation function along vertical directions. For example, to calculate the correlation function of  $S^x$ , we fix the magnetic order along the  $y$ -direction on the isotropic line. It is noteworthy that the effective correlation length  $\xi$  is the intrinsic characteristic of a wave function and will not be influenced by the direction of the magnetic order.

#### 4. Numerical Analysis of the KT Transition

To accurately locate the location of the tricritical point, the most convenient way is to approach it along the isotropic line ( $J_x = J_y$ ). In this situation, the sine-Gordon model has predicted that the system will undergo a KT transition from the Luttinger liquid phase to an ordered phase. We first examine the behaviors of the Luttinger liquid to VBS transition. For simplicity, we ignore the  $x, y$  indices and label  $J_x = J_y$  as  $J$  in the following sections.



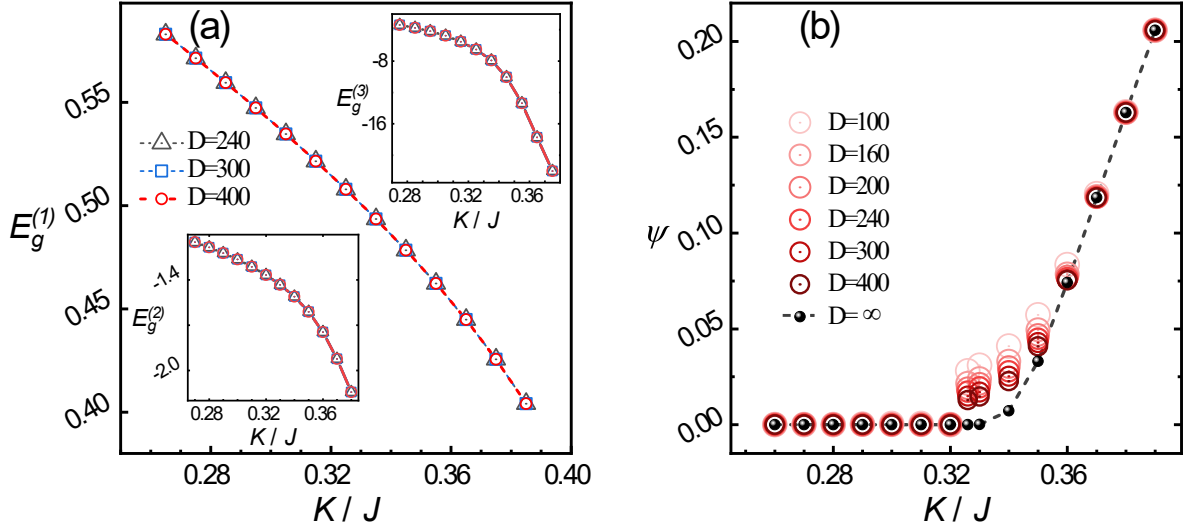
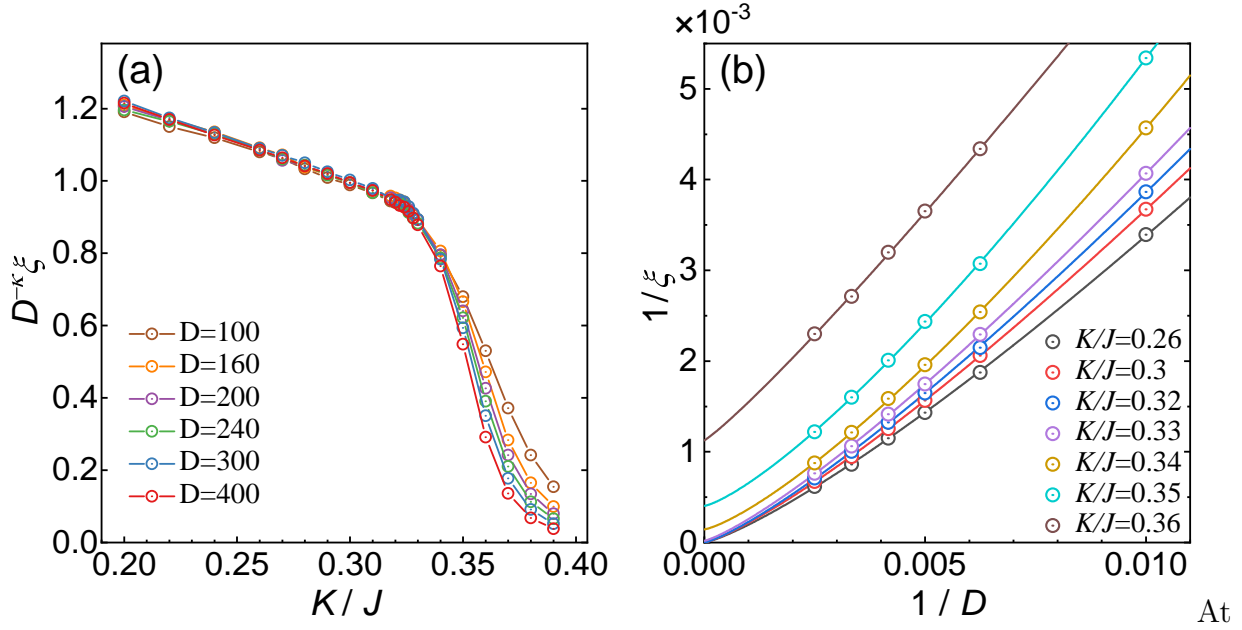


**Figure 2.** (a) The first derivative  $E_g^{(1)}$  of the ground-state energy with  $K/J$  along the blue line in Fig. 1. The inserts show the second derivative  $E_g^{(2)}$  and third derivative  $E_g^{(3)}$  of the ground-state energy, respectively. (b) The VBS order parameter  $\psi$  with  $K/J$ .

The VBS order parameter  $\psi = \sum_j (-1)^j \vec{S}_j \vec{S}_{j+1}$  has been calculated. As shown in Fig. 2(b),  $\psi$  exhibits a near-continuous transition at the point about  $K/J \approx 0.324$ . As the parameter  $K/J$  approaches the transition point from the VBS order phase, the split of  $\psi$  for different  $D$  becomes more obvious, which means a notable finite- $D$  effect. To eliminate the finite- $D$  effect and obtain the behavior of order parameters in the thermodynamic limit, we extrapolate their values in the large- $D$  limit, as also shown in Fig. 2(b). The extrapolated results of  $\psi$  for  $D = \infty$  exhibit a smooth and continuous transition. We further calculate the ground-state energy  $E_g$ , its first derivative  $E_g^{(1)} = dE_g/dK$ , the second derivative  $E_g^{(2)} = dE_g^{(1)}/dK$ , and the third derivative  $E_g^{(3)} = dE_g^{(2)}/dK$  to explore the transition. As demonstrated in Fig. 2(a), all these derivatives vary continuously across the transition, and do not develop a singularity or discontinuity. This is consistent with a KT transition, which is an infinite-order transition.

To obtain more convincing evidence for the KT transition and determine the exact location of the transition point, we calculate the effective correlation length  $\xi$  for different  $D$ . As demonstrated in Fig. 3 (a),  $\xi$  varies smoothly for small  $K$ , and rapidly decay for  $K/J \gtrsim 0.33$ , featuring a process from a gapless system to a gapped system. The transition point can be determined by the kink to be  $K_c/J \approx 0.323 \pm 0.002$ . With properly choosing the exponent  $\kappa \approx 1.23$ , all  $\xi$  data collapse when the system is gapless. The exponent  $\kappa$  is a universal constant related to the central charge  $c$  of the system. The  $\kappa$  value we obtained is close to the predicted one,  $\kappa \approx 1.334$ , for a system with central charge  $c = 1$ . [34, 52] Direct and clear results are also shown in Fig. 3 (b). The results for  $K/J \leq 0.32$  can all be fitted by power law functions with  $\kappa \approx 1.23$  which is close to



the tricritical point, the system is marginal to be a  $n_1$  orderd, a  $n_2$  orderd or a  $n_3$  phase.

**Figure 3.** (a) Scaling of the effective correlation length  $\xi$  with  $K/J$  across the KT transition point along the blue line in Fig. 1 for different  $D$ . (b) Scaling of  $1/\xi$  as a function of  $1/D$  for different  $K/J$ .

the predictive value of 1.344. However, for the gapped system, it is expected to observe a finite value of  $\xi$  even in the  $D = \infty$  limit. The results for  $K/J \geq 0.34$  in Fig. 3 (b) can not be fitted by power functions without a constant term and the extrapolations of  $\xi$  for these results in the  $D = \infty$  limit are all finite values. These results evidence a KT transition for  $0.32 \lesssim K/J \lesssim 0.33$ .

The transition point can also be determined more accurately by another method. At the tricritical point, the sine-Gordon model has predicted that a multiplicative logarithmic correction term  $|\ln(r)|^{1/2}$  appears in the correlation functions as mentioned in Eq. 11. As demonstrated in Fig. 4, we plot  $rG_{x/y}$  and  $rG_\psi$  as a function of  $|\ln(r)|^{1/2}$  for different  $K/J$ . Here  $G_u = \langle u(0)u(r) \rangle - \langle u \rangle^2$ . Exactly at the tricritical point, both of these two plots will be linear. The following work becomes to decide which one of the these curves is closer to the perfect linear dependence. By combing the results of Fig. 4 (a) and (b), we determine the transition point is between  $K/J = 0.322$  to  $K/J = 0.324$ . This result in consistent with above two methods, and it is also consistent with the estimates in previous works [38, 54].

## 5. Numerical Evidence of Emergent $O(4)$ Symmetry

In this section we prove the existence of an enhanced  $O(4)$  symmetry by calculating the exponents  $\eta$  of the  $O(4)$  pseudovector components related by the emergent symmetry and the associated emergent conserved currents. There will be two sets of evidences

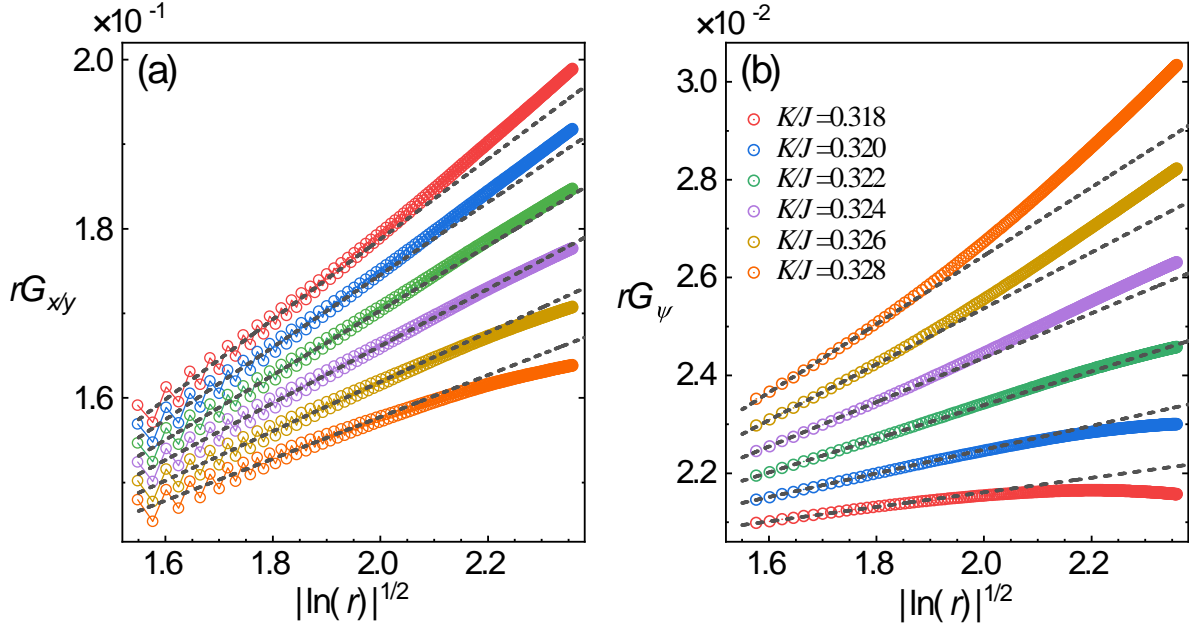


**Figure 4.** (a)  $rG_{x/y}$  and (b)  $rG_{\psi}$  as a function of  $|\ln(r)|^{1/2}$  for different  $K/J$ .  $G_{x/y}$  and  $G_{\psi}$  are the correlation functions of  $S_{x/y}$  and  $\psi$ , respectively. The dashed linear lines are guides to eyes.

for the existence of the enhanced  $O(4)$  symmetry. The first evidence is that the critical behaviors and exponents  $\eta$  of the vector components are all in accord with the theoretical predictions of the WZNW model, which holds an  $SU(2) \times SU(2) \sim O(4)$  symmetry. The other robust evidence is that  $\eta$  of all associated emergent conserved currents are pinned to the integer value 2.

The effective correlation length  $\xi$  has been calculated in Sec 4. All  $\xi$  values for the gapless system are larger than 1400 with  $D = 400$ , and we fit the data up to about  $r \lesssim 1000$ , which is reliable.

We first estimate  $\eta$  of vector components by fitting correlation functions for different  $K/J$ . As shown in Fig. 5(a), the  $\eta$  of  $n_1$ ,  $n_2$ , and  $n_4$  at the tricritical point are identical and close to the integer 1. But the  $\eta$  values of  $n_3$  and  $n_4$  differs when the system is close to the tricritical point. By comparing the  $D = 400$  data with those of  $D = 100$ , we clearly show that this is a finite- $D$  effect, which lies in the microscopic model because the marginal irrelevance only strictly holds in the thermodynamic limit (infrared limit). For finite- $D$  systems, corrections that are relevant always exist. At the tricritical point, the system is marginal to be in either a  $n_1$  ordered, or a  $n_2$  ordered, or a  $n_3$  ordered phase. Therefore,  $n_4$  is more *relevant* than  $n_3$  in short range. Nevertheless, in the infrared limit, this two  $\eta$  will both flow to 1, as suggested by the finite- $D$  study in Fig. 5 (a).

The correlation-function exponents of the emergent conserved currents are also estimated. As demonstrated in Fig. 5(b), the evidences from  $\eta$  of conserved currents are more robust. The  $\eta$  of all conserved currents at the tricritical points are identical

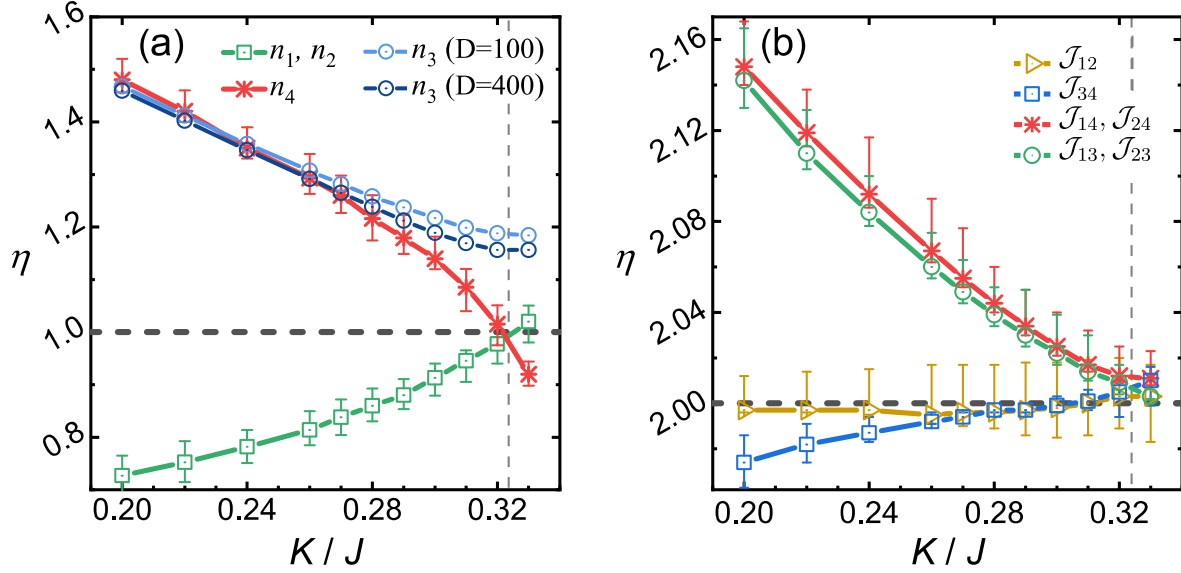


**Figure 5.** The exponent  $\eta$  of the O(4) pseudovector components (in (a)) and associated conserved currents (in (b)) with  $K/J$ . Constrained by the LSM theorem, the ground state should preserve the rotational symmetry between  $S_x(n_1)$  and  $S_y(n_2)$ . Hence, the results of interchanging the indices  $1 \leftrightarrow 2$  are identical in the calculation.

to be 2. Another interesting result shown in Fig. 5(b) is that the  $\eta$  approximately keeps symmetric for  $J_{12} \leftrightarrow J_{34}$ ,  $J_{13} \leftrightarrow J_{24}$ , and  $J_{14} \leftrightarrow J_{23}$  interchange. It reflects a space-time duality of the conserved currents.

To further show the evidence of the emergent O(4) symmetry clearly, we calculate the correlation functions of vector components and associated emergent conserved currents just at the tricritical point ( $J_x = J_y$ ,  $K/J = 0.322$ ) as shown in Fig. 6. The dashed lines in Fig. 6(a) are guide lines with  $\eta = 2$ . All these emergent conserved currents are in accord with the expected behaviors of  $\eta = 2$  very well. The exponents of these 4 vector components in Fig. 6(b) are approximately equal, signaling the O(4) symmetry.

## 6. Discussions and Conclusions

As mentioned in the introduction, the origin of emergent enhanced continuous symmetry at the transition point is still challenging. In this work, we systematically investigate the enhanced O(4) symmetry on a 1D tricritical point. We justify the emergence of this symmetry by combining analytical analysis with numerical calculations. Note that the exact symmetry only exist in the infrared limit, which is usually difficult for numerics. To address this issue numerically, employ the iTEBD method to study the ground-state properties of the system. We verify the emergent symmetry by two sets of evidences: checking the critical exponents with the symmetry-enhanced low-energy effective theory, and verifying if the scaling dimensions of conserved currents are pinned to an integer. The agreement between numerical and analytical results indicates the numerical method

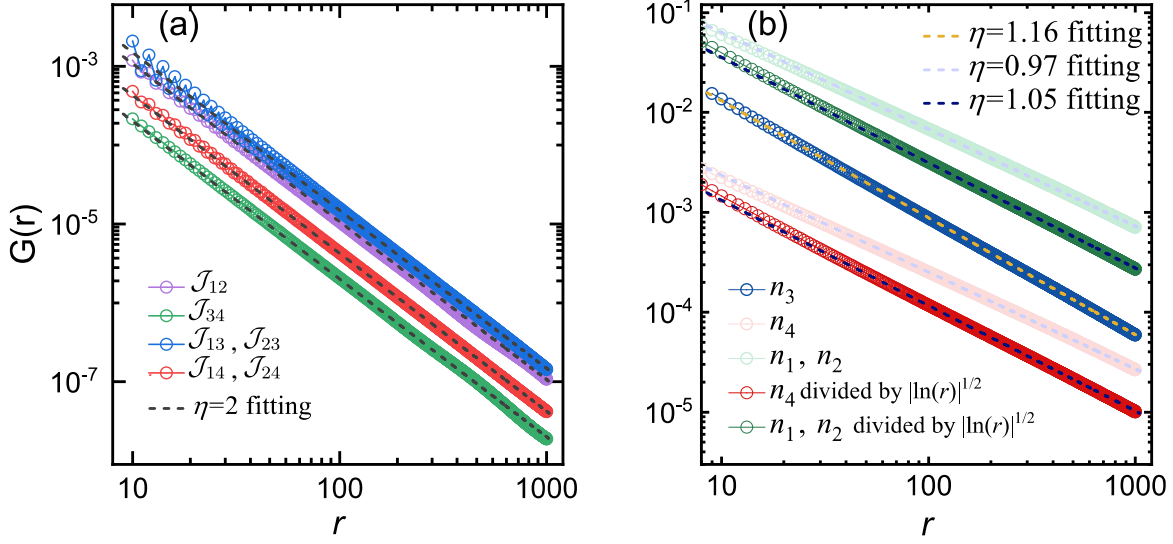


**Figure 6.** Correlation functions of (a) emergent conserved currents and (b) vector components at the tricritical point.

is capable of handling this issue. Application of our method to other problems would be interesting. Note that our method also provides a new approach to study the KT transition numerically.

For this specific model, the marginally irrelevant terms result in that the system only keep the enhanced  $O(4)$  symmetry in the infrared limit. But an extended  $SU(2) \times U(1)$  symmetry still preserves in the short length scale. As an extension of this work, if we consider a global phase diagram with an extra tuning parameter, such as an AFM exchange coupling along  $S^z$ , enhanced  $O(4)$  symmetry at some transition points may be more general.

In higher dimensions, verifying the emergent symmetry by conserved currents at DQCPs has been applied to some systems [25, 27]. Besides a deconfined transition, emergent symmetry in higher dimensions may be even of first order, where the emergent Goldstone mode associated with the enhanced symmetry appears at the transition. In this case, the system keeps gapless at the first-order transition, and the analysis based on exponents of correlation functions in our method will still be applicable.

## References

- [1] Subir Sachdev. *Quantum phase transitions*. Cambridge university press, 2011.
- [2] Thierry Giamarchi. *Quantum Physics in One Dimension*, volume 121. Oxford University Press, 2004.
- [3] Eduardo Fradkin. *Field theories of condensed matter physics*. Cambridge University Press, 2013.
- [4] Paul M Chaikin, Tom C Lubensky, and Thomas A Witten. *Principles of condensed matter physics*, volume 10. Cambridge university press Cambridge, 1995.
- [5] Alexei M Tsvelik. *Quantum field theory in condensed matter physics*. Cambridge university press, 2007.

- [6] Naoto Nagaosa. *Quantum field theory in strongly correlated electronic systems*. Springer Science & Business Media, 1999.
- [7] Claudine Lacroix, Philippe Mendels, and Frédéric Mila. *Introduction to frustrated magnetism: materials, experiments, theory*, volume 164. Springer Science & Business Media, 2011.
- [8] HT Diep et al. *Frustrated spin systems*. World Scientific, 2013.
- [9] Leon Balents. Spin liquids in frustrated magnets. *Nature*, 464(7286):199–208, 2010.
- [10] Hui Shao, Wenan Guo, and Anders W. Sandvik. Quantum criticality with two length scales. *Science*, 352(6282):213–216, 2016.
- [11] R. Coldea, D. A. Tennant, E. M. Wheeler, E. Wawrzynska, D. Prabhakaran, M. Telling, K. Habicht, P. Smeibidl, and K. Kiefer. Quantum criticality in an ising chain: Experimental evidence for emergent  $U(1)$  symmetry. *Science*, 327(5962):177–180, 2010.
- [12] Shou-Cheng Zhang. A unified theory based on  $U(1)$  symmetry of superconductivity and antiferromagnetism. *Science*, 275(5303):1089–1096, 1997.
- [13] T. Senthil, Ashvin Vishwanath, Leon Balents, Subir Sachdev, and Matthew P. A. Fisher. Deconfined quantum critical points. *Science*, 303(5663):1490–1494, Mar 2004.
- [14] Adam Nahum, P. Serna, J. T. Chalker, M. Ortuño, and A. M. Somoza. Emergent  $so(5)$  symmetry at the néel to valence-bond-solid transition. *Phys. Rev. Lett.*, 115:267203, Dec 2015.
- [15] Snir Gazit, Fakher F. Assaad, Subir Sachdev, Ashvin Vishwanath, and Chong Wang. Confinement transition of  $z_2$  gauge theories coupled to massless fermions: Emergent quantum chromodynamics and  $so(5)$  symmetry. *Proceedings of the National Academy of Sciences*, 115(30):E6987–E6995, 2018.
- [16] Bowen Zhao, Phillip Weinberg, and Anders W Sandvik. Symmetry-enhanced discontinuous phase transition in a two-dimensional quantum magnet. *Nature Physics*, 15(7):678–682, 2019.
- [17] Haiyuan Zou, Yi Cui, Xiao Wang, Z. Zhang, J. Yang, G. Xu, A. Okutani, M. Hagiwara, M. Matsuda, G. Wang, Giuseppe Mussardo, K. Hódsági, M. Kormos, Zhangzhen He, S. Kimura, Rong Yu, Weiqiang Yu, Jie Ma, and Jianda Wu.  $E_g$  spectra of quasi-one-dimensional antiferromagnet  $\text{BaCo}_2\text{V}_2\text{O}_8$  under transverse field. *Phys. Rev. Lett.*, 127:077201, Aug 2021.
- [18] Y. Cui, H. Zou, N. Xi, Zhangzhen He, Y. X. Yang, L. Shu, G. H. Zhang, Z. Hu, T. Chen, Rong Yu, Jianda Wu, and Weiqiang Yu. Quantum criticality of the ising-like screw chain antiferromagnet  $\text{SrCo}_2\text{V}_2\text{O}_8$  in a transverse magnetic field. *Phys. Rev. Lett.*, 123:067203, Aug 2019.
- [19] Jong Yeon Lee, Yi-Zhuang You, Subir Sachdev, and Ashvin Vishwanath. Signatures of a deconfined phase transition on the shastry-sutherland lattice: Applications to quantum critical  $\text{SrCu}_2(\text{BO}_3)_2$ . *Phys. Rev. X*, 9:041037, Nov 2019.
- [20] Cui Yi and et al. Proximate deconfined quantum critical point in the shastry-sutherland material, 2021.
- [21] Ning Xi, Hongyu Chen, Z. Y. Xie, and Rong Yu. First-order transition between the plaquette valence bond solid and antiferromagnetic phases of the shastry-sutherland model, 2021.
- [22] T. Senthil, Leon Balents, Subir Sachdev, Ashvin Vishwanath, and Matthew P. A. Fisher. Quantum criticality beyond the landau-ginzburg-wilson paradigm. *Phys. Rev. B*, 70:144407, Oct 2004.
- [23] Anders W. Sandvik. Evidence for deconfined quantum criticality in a two-dimensional heisenberg model with four-spin interactions. *Phys. Rev. Lett.*, 98:227202, Jun 2007.
- [24] Kun Chen, Yuan Huang, Youjin Deng, A. B. Kuklov, N. V. Prokof'ev, and B. V. Svistunov. Deconfined criticality flow in the heisenberg model with ring-exchange interactions. *Phys. Rev. Lett.*, 110:185701, May 2013.
- [25] Nvsen Ma, Yi-Zhuang You, and Zi Yang Meng. Role of noether's theorem at the deconfined quantum critical point. *Phys. Rev. Lett.*, 122:175701, May 2019.
- [26] Yan Qi Qin, Yuan-Yao He, Yi-Zhuang You, Zhong-Yi Lu, Arnab Sen, Anders W. Sandvik, Cenke Xu, and Zi Yang Meng. Duality between the deconfined quantum-critical point and the bosonic topological transition. *Phys. Rev. X*, 7:031052, Sep 2017.
- [27] Nvsen Ma, Guang-Yu Sun, Yi-Zhuang You, Cenke Xu, Ashvin Vishwanath, Anders W. Sandvik, and Zi Yang Meng. Dynamical signature of fractionalization at a deconfined quantum critical

- point. *Phys. Rev. B*, 98:174421, Nov 2018.
- [28] Yan Qi Qin, Yuan-Yao He, Yi-Zhuang You, Zhong-Yi Lu, Arnab Sen, Anders W. Sandvik, Cenke Xu, and Zi Yang Meng. Duality between the deconfined quantum-critical point and the bosonic topological transition. *Phys. Rev. X*, 7:031052, Sep 2017.
  - [29] Chong Wang, Adam Nahum, Max A. Metlitski, Cenke Xu, and T. Senthil. Deconfined quantum critical points: Symmetries and dualities. *Phys. Rev. X*, 7:031051, Sep 2017.
  - [30] Elliott Lieb, Theodore Schultz, and Daniel Mattis. Two soluble models of an antiferromagnetic chain. *Annals of Physics*, 16(3):407–466, 1961.
  - [31] Kiyohide Nomura, Junpei Morishige, and Takaichi Isoyama. Extension of the lieb–schultz–mattis theorem. *Journal of Physics A: Mathematical and Theoretical*, 48(37):375001, aug 2015.
  - [32] Takaichi Isoyama and Kiyohide Nomura. Discrete symmetries and the lieb–schultz–mattis theorem. *Progress of Theoretical and Experimental Physics*, 2017(10), 10 2017. 103I01.
  - [33] Christopher Mudry, Akira Furusaki, Takahiro Morimoto, and Toshiya Hikihara. Quantum phase transitions beyond landau-ginzburg theory in one-dimensional space revisited. *Phys. Rev. B*, 99:205153, May 2019.
  - [34] Rui-Zhen Huang, Da-Chuan Lu, Yi-Zhuang You, Zi Yang Meng, and Tao Xiang. Emergent symmetry and conserved current at a one-dimensional incarnation of deconfined quantum critical point. *Phys. Rev. B*, 100:125137, Sep 2019.
  - [35] Rui-Zhen Huang and Shuai Yin. Kibble-zurek mechanism for a one-dimensional incarnation of a deconfined quantum critical point. *Phys. Rev. Research*, 2:023175, May 2020.
  - [36] Brenden Roberts, Shenghan Jiang, and Olexei I. Motrunich. Deconfined quantum critical point in one dimension. *Phys. Rev. B*, 99:165143, Apr 2019.
  - [37] Shenghan Jiang and Olexei Motrunich. Ising ferromagnet to valence bond solid transition in a one-dimensional spin chain: Analogies to deconfined quantum critical points. *Phys. Rev. B*, 99:075103, Feb 2019.
  - [38] Shunsuke Furukawa, Masahiro Sato, Shigeki Onoda, and Akira Furusaki. Ground-state phase diagram of a spin- $\frac{1}{2}$  frustrated ferromagnetic xxz chain: Haldane dimer phase and gapped/gapless chiral phases. *Phys. Rev. B*, 86:094417, Sep 2012.
  - [39] Sheng Yang and Jing-Bo Xu. Quantum entanglement and criticality in a one-dimensional deconfined quantum critical point. *Phys. Rev. E*, 104:064121, Dec 2021.
  - [40] Christopher Mudry, Akira Furusaki, Takahiro Morimoto, and Toshiya Hikihara. Quantum phase transitions beyond landau-ginzburg theory in one-dimensional space revisited. *Physical Review B*, 99(20):205153, 2019.
  - [41] Pranay Patil, Emanuel Katz, and Anders W. Sandvik. Numerical investigations of  $so(4)$  emergent extended symmetry in spin- $\frac{1}{2}$  heisenberg antiferromagnetic chains. *Phys. Rev. B*, 98:014414, Jul 2018.
  - [42] Sibin Yang, Dao-Xin Yao, and Anders W. Sandvik. Deconfined quantum criticality in spin-1/2 chains with long-range interactions, 2020.
  - [43] I. Affleck. Critical behavior of two-dimensional systems with continuous symmetries. *Phys. Rev. Lett.*, 55:1355–1358, Sep 1985.
  - [44] Ian Affleck and F. D. M. Haldane. Critical theory of quantum spin chains. *Phys. Rev. B*, 36:5291–5300, Oct 1987.
  - [45] Ning Xi and Rong Yu. Dynamical signatures of the one-dimensional deconfined quantum critical point, 2022.
  - [46] Ian Affleck. Exact correlation amplitude for the heisenberg antiferromagnetic chain. *Journal of Physics A: Mathematical and General*, 31(20):4573–4581, may 1998.
  - [47] A. Luther and I. Peschel. Calculation of critical exponents in two dimensions from quantum field theory in one dimension. *Phys. Rev. B*, 12:3908–3917, Nov 1975.
  - [48] Toshiya Hikihara, Akira Furusaki, and Sergei Lukyanov. Dimer correlation amplitudes and dimer excitation gap in spin- $\frac{1}{2}$  xxz and heisenberg chains. *Phys. Rev. B*, 96:134429, Oct 2017.
  - [49] G. Vidal. Classical simulation of infinite-size quantum lattice systems in one spatial dimension.

- Phys. Rev. Lett.*, 98:070201, Feb 2007.
- [50] Ulrich Schollwöck. The density-matrix renormalization group in the age of matrix product states. *Annals of Physics*, 326(1):96–192, 2011. January 2011 Special Issue.
  - [51] L. Tagliacozzo, Thiago. R. de Oliveira, S. Iblisdir, and J. I. Latorre. Scaling of entanglement support for matrix product states. *Phys. Rev. B*, 78:024410, Jul 2008.
  - [52] Frank Pollmann, Subroto Mukerjee, Ari M. Turner, and Joel E. Moore. Theory of finite-entanglement scaling at one-dimensional quantum critical points. *Phys. Rev. Lett.*, 102:255701, Jun 2009.
  - [53] B. Pirvu, G. Vidal, F. Verstraete, and L. Tagliacozzo. Matrix product states for critical spin chains: Finite-size versus finite-entanglement scaling. *Phys. Rev. B*, 86:075117, Aug 2012.
  - [54] K Nomura and K Okamoto. Critical properties of  $s=1/2$  antiferromagnetic XXZ chain with next-nearest-neighbour interactions. *Journal of Physics A: Mathematical and General*, 27(17):5773–5788, sep 1994.